JOURNAL OF MATERIALS SCIENCE **36** (2001) 5391 – 5395

Size effect of trivalent oxides on low temperature phase stability of 2Y-TZP

JU-WOONG JANG
Dental Material Research Center, We Dong Myung Co. Ltd., Kwangmyung 423-060, Korea
DAE-JOON KIM
Materials Division, Korea Institute of Science and Technology, Seoul 136-791, Korea
DEUK YONG LEE*
Department of Materials Engineering, Daelim College of Technology, Anyang 431-715, Korea
E-mail: dylee@daelim.ac.kr

2 mol% Y_2O_3 stabilized-TZPs (2Y-TZPs) doped with oversized trivalent cations ($Sc^{3+} < Yb^{3+} < Y^{3+} < Sm^{3+} < Nd^{3+} < La^{3+}$) whose ionic radius is larger than Zr^{4+} was sintered for 1 h at 1500°C over the range containing trivalent oxides from 0 to 2 mol% with 0.5 mol% interval to evaluate the effect of trivalent cation alloying on low temperature phase stability of 2Y-TZP by investigating the variation of Raman spectra and lattice parameters. For a given concentration of dopant, tetragonality (*c*/*a* axial ratio) increases with raising the dopant size. However, monoclinic (m)-ZrO_2 content for the specimens annealed for 500 h at 220°C in air firstly decreases with increasing dopant size and then increases as dopant size is greater than Y^{3+} ion. Raman modes of Zr-O_{II} (260 cm^{-1}) and Zr-O_I (640 cm^{-1}) shift to higher wavenumbers only when Sm_2O_3, Nd_2O_3, and La_2O_3 are added. Although full width at half maximum (FWHM) of 640 cm^{-1} is constant, FWHM of 260 cm^{-1} mode decreases with increasing dopant size, indicating that an ordered structure (pyrochlore phase) may be formed. Therefore, dopant size is dependent on phase stability of 2Y-TZP in this system.

1. Introduction

Trivalent cation alloying having greater ionic size than Zr^{4+} to tetragonal zirconia polycrystals (TZPs) is known to serve as t- and cubic (c)-ZrO_2 phase stabilizer because substitution causes distorted fluorite structure and oxygen vacancy due to the ionic size and the charge deficiency [1, 2]. Vacancies formed by the substitution of oversized trivalent dopants for Zr^{4+} are positioned as nearest neighbors to Zr atoms, leaving 8-fold oxygen coordination to dopant cations [3]. Therefore, internal strain inherent in the t-lattice caused by smaller ionic size of Zr^{4+} is relieved by the presence of oxygen vacancies associated with Zr and oversized dopants, resulting in retention of low temperature degradation (LTD). It is reported that stabilization of high-temperature polymorphs of zirconia depends on cation size, cation concentration, number of oxygen vacancies, and crystal structure of dopant [3–5].

In zirconia solid solutions with oversized trivalent dopants, tetragonality (c/a axial ratio), associated with the internal strain, decreases with increasing dopant concentration, representing that the loss of tetragonality is correlated with increased stability against t → m phase transformation. Yoshimura and Yashima [6] reported that the c/a ratio is independent of the dopant size, but dependent on the content of dopants in the ZrO_2-$RO_{1.5}$ (R = Nd, Sm, Er, Yb, Sc) systems. In the present study, 2Y-TZP doped with oversized trivalent dopants (Sc^{3+}, Yb^{3+}, Y^{3+}, Sm^{3+}, Nd^{3+}, La^{3+}) was synthesized by sintering over the composition range containing trivalent oxides from 0 to 2 mol% with 0.5 mol% interval to evaluate the effect of trivalent cation alloying on low temperature phase stability and tetragonality of 2Y-TZP by using Raman spectroscopy and X-ray diffractometer (XRD).

2. Experimental procedure

Zirconia solid solutions with trivalent oxides from 0 to 2 mol% with 0.5 mol% interval were prepared by using 2Y-TZP (Tosoh Inc., Japan), Sc_2O_3 (Aldrich Inc., USA), Yb_2O_3 (Aldrich Inc., USA), Y_2O_3 (Aldrich Inc., USA), Sm_2O_3 (Aldrich Inc., USA), Nd_2O_3 (Aldrich Inc., USA), and La_2O_3 (Aldrich Inc., USA) as the starting powders. The powders were mixed by ball mill with zirconia balls for 24 h. After drying, the mixed powders

*Author to whom all correspondence should be addressed.

TABLE I Ionic radius and Ionic radius difference at 8-coordinate

Ion	Ionic Radius($r_M{}^{3+}$) (Å)	Δr ($r_M{}^{3+} - r_{Zr}{}^{4+}$) (Å)
Sc^{3+}	0.87	0.03
Yb^{3+}	0.985	0.145
Y^{3+}[9]	1.011	0.175
Sm^{3+}	1.079	0.239
Nd^{3+}	1.109	0.269
La^{3+}	1.16	0.32

were calcined for 4 h at 1100°C followed by attrition milling for 1 h. Pellets of each composition were isostatically pressed at 140 MPa and then sintered for 1 h at 1500°C.

The samples were aged for 500 h at 220°C and then the extent of low temperature degradation (LTD) was estimated from the m-ZrO_2 fraction of the aged specimens according to Garvie and Nicholson [7] using XRD.

Thermal etching was performed for 12 min at 1450°C before microstructural observation using scanning electron microscopy (SEM). The linear intercept method was used to determine the average grain size with the use of correction factor of 1.56 after Mendelson [8]. Thermal gravity and differential thermal analysis (TG/DTA-92, Setaram. France) were performed at temperatures from room temperature to 1200°C with a heating rate of 10°C/min for the determination of t → m phase transformation temperature.

For the determination of lattice parameter at room temperature, XRD data were obtained from the ground powders, mixed carefully with the silicon internal standard (SRM 640b, National Institute of Standards and Technology, Gaithersburg, MD), using an automated XRD (Phillips, EA, Almelo, The Netherlands) with Cu K_α radiation. A scan speed of 0.5° 2θ/min was used in the 2θ range of 65° to 120°. After kα2 peak stripping, the peak position was determined by profile refinement using the built-in PC-APD program [9].

Raman spectra were obtained by a double monochromater (U1000, Jobin Yvon, Longjumeau, France) in a backscattering geometry. The spectra were excited with an argon ion laser that was operating at a wavelength of 514.5 nm. Spectra each specimen were taken over the range of 100–900 cm^{-1}, scanning at a step size of 1.0 cm^{-1} with an integration time constant of 1 s. The instrument was calibrated with the 520.9 cm^{-1} Raman band of silicon wafer, and the error in determining the peak shifts was ±1 cm^{-1}. The wavenumbers of the Raman bands were determined by the Lorentzian curve fitting of the spectra [10].

3. Results and discussion

Ionic radii of trivalent dopants for 8-fold coordination given by Shannon [11] and Kim (Y^{+3}) [9] are summarized in Table I. Oversized trivalent cations are only considered in the present study because oversized dopants is likely to relieve the internal strain caused by smaller ionic size of Zr^{4+} (0.84 Å) for stabilization of t- and c-ZrO_2 phase. The difference in ionic radius of the

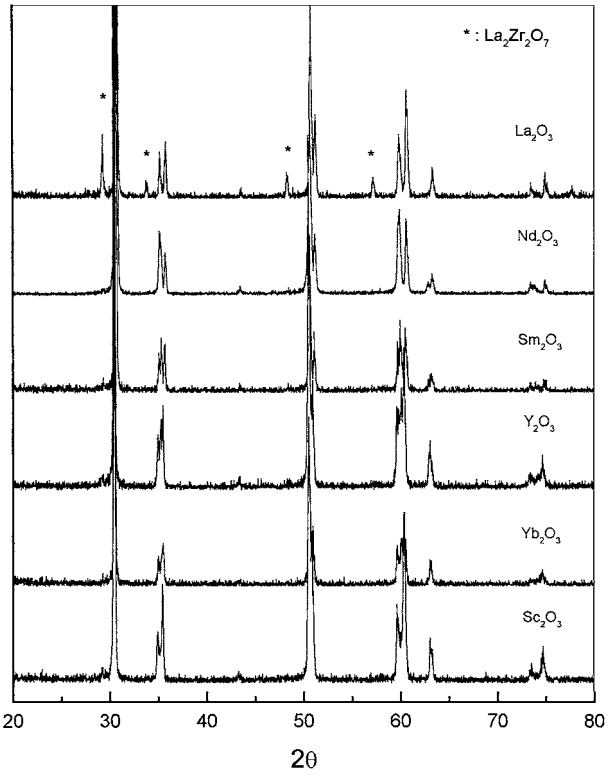

Figure 1 XRD patterns of 2Y-TZP doped with 0.5 mol% M_2O_3 (M = Sc, Yb, Y, Sm, Nd, La).

dopant cation and the host cation (Zr^{4+}) ranges from 0.03 Å(Sc^{3+}, 0.87 Å) to 0.32 Å(La^{3+}, 1.16 Å). According to phase diagrams [12–16], it is expected that pyrochlore phase may be formed instead of t- or c-ZrO_2 phase since solid solubility region of t- and c-ZrO_2 in the binary systems ZrO_2-M_2O_3 (M = Sm_2O_3, Nd_2O_3, La_2O_3) becomes narrower as the ionic size mismatch and the dopant concentration become greater. XRD results of Fig. 1 showed that t-ZrO_2 was stable for 2Y-TZPs doped with up to 2 mol% Sc_2O_3, however, pyrochlore phase was observed for 2Y-TZPs doped with more than 0.5 mol% La_2O_3 due to the limited solid solubility. As dopants concentration (Yb, Y, Sm, Nd) whose ionic size is located between Sc and La increases, the fraction of c-ZrO_2 increases as shown in Fig. 2. Therefore, XRD results indicate that three types of phases (t-ZrO_2, c-ZrO_2, pyrochlore) may become stable depending on dopant species and concentration.

Low temperature phase stability was determined by measuring m-ZrO_2 content of the aged 2Y-TZPs doped with various dopants by using XRD. At low dopant concentration less than 0.5 mol%, the effect of dopant size on phase stability of 2Y-TZP was indistinguishable, however, the size effect became pronounced at dopant concentration more than 1 mol% as shown in Fig. 3. It is expected that oversized dopant alloying to 2Y-TZP may enhance the phase stability due to the decrease in internal strain as a result of dopant ionic size. However, low temperature phase stability of 2Y-TZP was firstly enhanced with raising dopant size and then degraded as dopant size was greater than Y^{3+} ion. Even though the content of c-ZrO_2 is reverse and the ionic size is greater than Y^{3+} ion as shown in Fig. 2 and Table I, phase stability of 2Y-TZP doped with more than 1 mol% Sm_2O_3

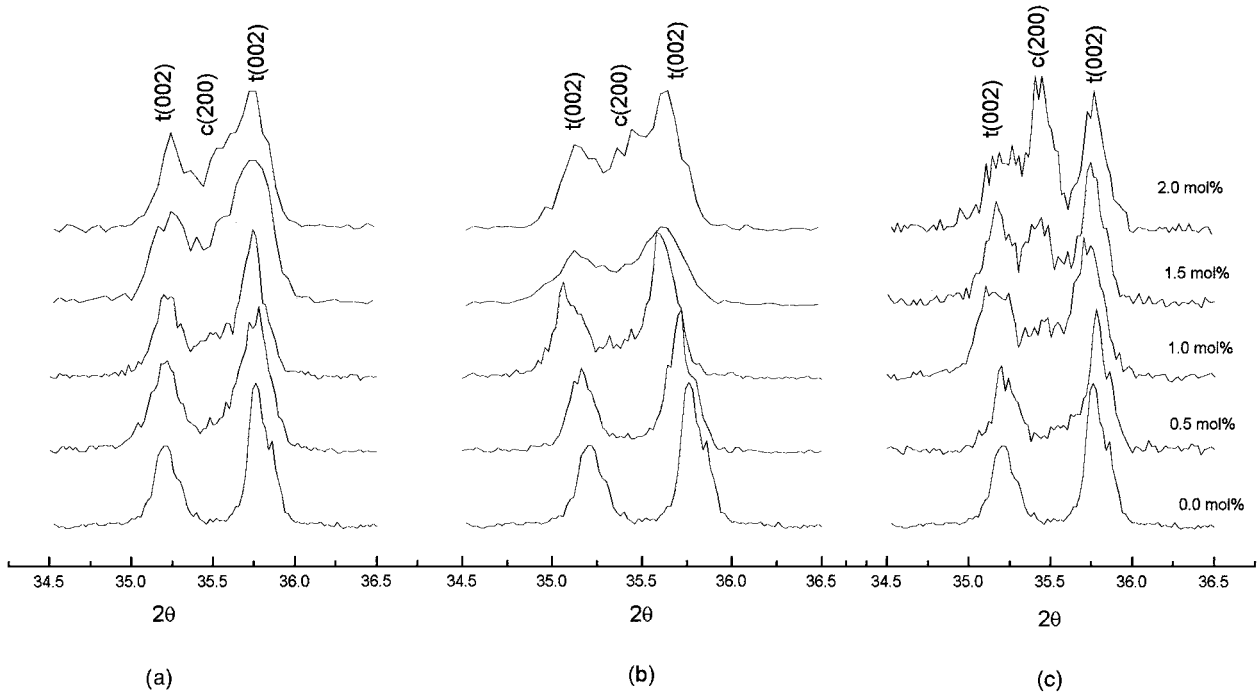

Figure 2 XRD patterns of 2Y-TZP doped with 0–2 mol% (a) Yb_2O_3, (b) Y_2O_3 and Sm_2O_3.

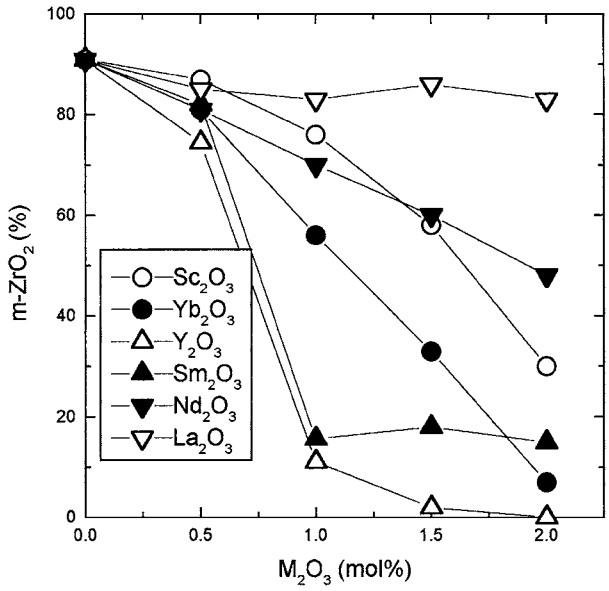

Figure 3 m-ZrO_2 content of 2Y-TZP doped with M_2O_3 (M = Sc, Yb, Y, Sm, Nd, La). The specimens were annealed for 500 h at 220°C in air.

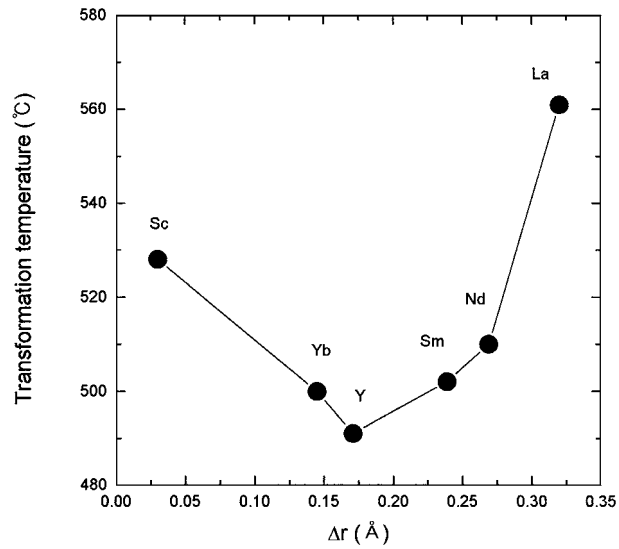

Figure 4 m → t phase transformation temperature of 2Y-TZP doped with 0.5 mol% M_2O_3 (M = Sc, Yb, Y, Sm, Nd, La).

was more hampered than that doped with Y_2O_3, indicating that there may exist a solubility limit and a critical ionic size for phase stability. Dopants whose ionic size is greater than Y^{3+} may be too big to form zirconia solid solution. Although XRD could not identify pyrochlore phase for 2Y-TZP doped with Sm_2O_3, it is expected that pyrochlore phase may be formed due to the ionic size mismatch.

Endothermal reaction related to t → m phase transformation temperature was determined by DTA/TG as shown in Fig. 4. Except La_2O_3 doped 2Y-TZP, t- and c-ZrO_2 phases only existed in this composition range and the content of c-ZrO_2 increased with increasing dopant size, suggesting that the transformation temperature should decrease with increasing dopant size. However, it is observed that transformation temperature of 2Y-TZP doped with Y_2O_3 was the lowest (491°C) and then increased again with increasing dopant size. This irrelevancy represents that there may exist a critical dopant ionic size for phase stability. The fraction of m-ZrO_2 formed on fracture surface of specimens showed the same trend as that of phase transformation temperature as shown in Fig. 5. In the present study, Y^{3+} ionic size is estimated to be mostly adequate for phase stability of 2Y-TZP.

The lattice parameters of 2Y-TZP are plotted as a function of the difference in ionic size of dopant and Zr as shown in Fig. 6. The lattice parameters of 2Y-TZP having the same content of dopant increase linearly with an increase in the size difference, but the effect of size difference on the *c*-axis lattice constant is more

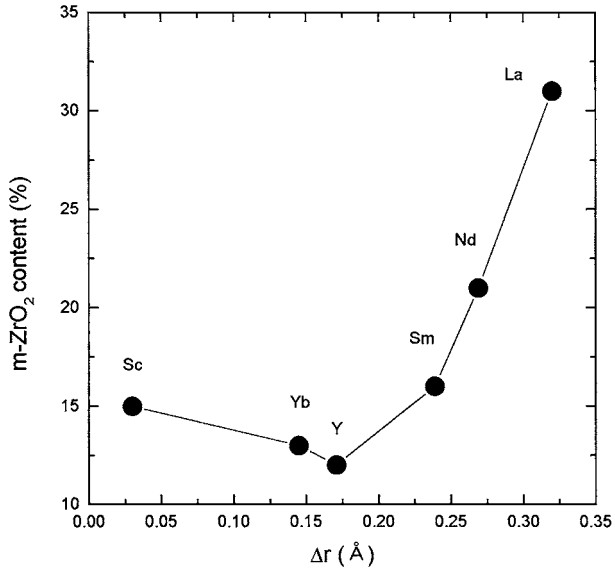

Figure 5 m-ZrO_2 content of the fractured surface of 2Y-TZP doped with 0.5 mol% M_2O_3 (M = Sc, Yb, Y, Sm, Nd, La).

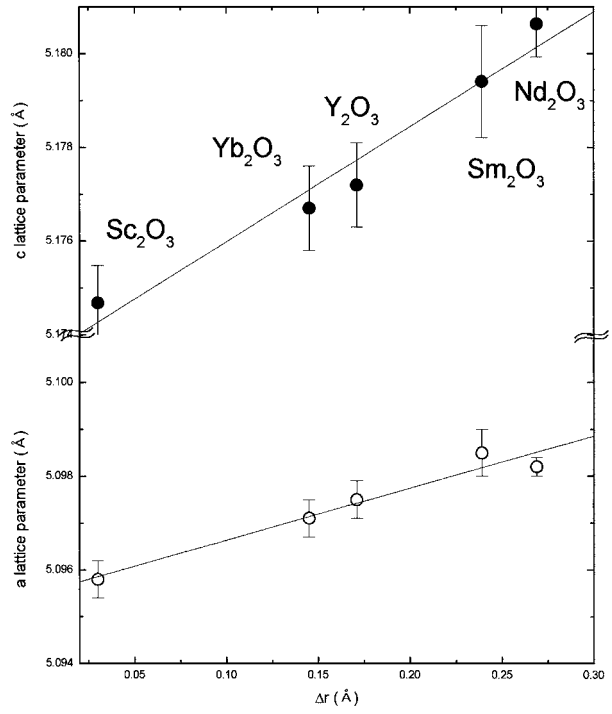

Figure 6 Lattice parameter of 2Y-TZP doped with 0.5 mol% M_2O_3 (M = Sc, Yb, Y, Sm, Nd, La).

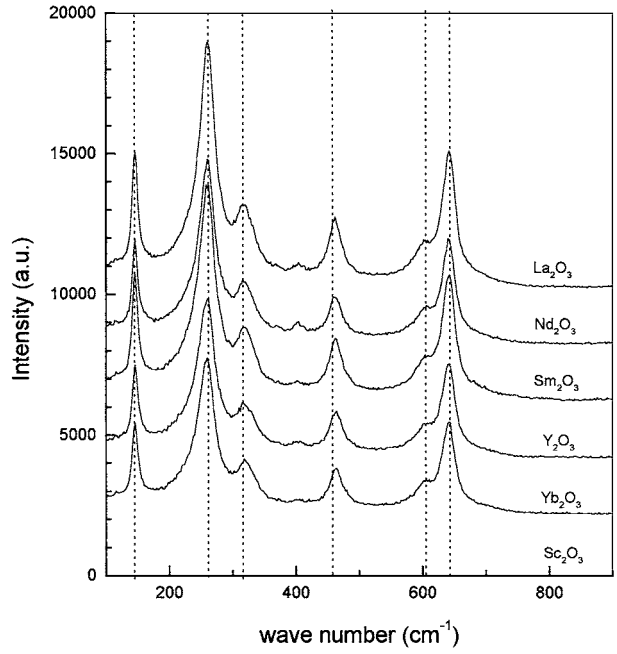

Figure 7 Raman spectra of 2Y-TZP doped with 0.5 mol% M_2O_3 (M = Sc, Yb, Y, Sm, Nd, La).

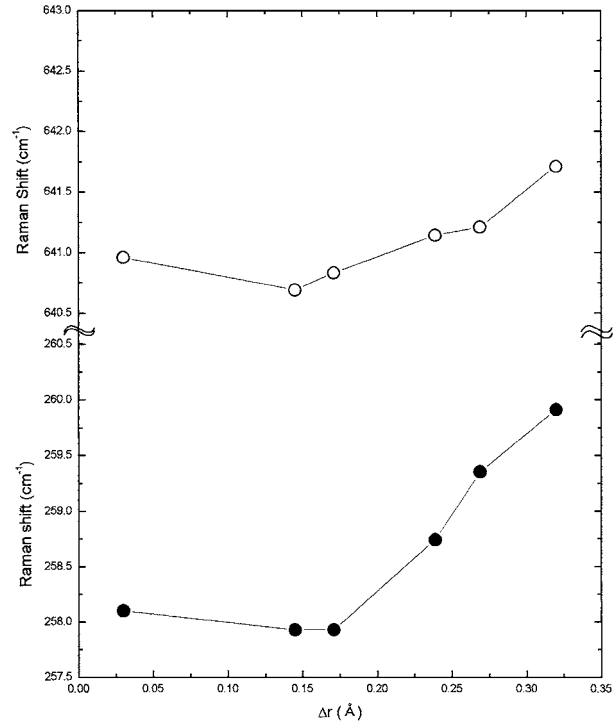

Figure 8 Raman shift of 260 cm^{-1} mode and 640 cm^{-1} mode of 2Y-TZP doped with 0.5 mol% M_2O_3 (M = Sc, Yb, Y, Sm, Nd, La).

pronounced compared with the changes in the a-axis lattice parameter. This observation is consistent with the result given by Lefevre [17]. Yohimura and Yashima [6] reported that the c/a ratio is independent of the dopant size, but dependent on the dopant concentration. That is, the a- and c-axis lattice parameters increase and decrease, respectively, as the dopant concentration rises. For a fixed concentration of dopants except Sc, the c/a ratio, however, also increases as the dopant size increases, which is consistent with our studies. Thus, the c/a ratio is dependent on the dopant size under the same amount of dopant, indicating that the c/a ratio is not a function of phase stability in this system. This reveals that the solubility of dopants to 2Y-TZP whose ionic size difference is above 0.239 Å is so limited that they may form the ordered structure (pyrochlore phase) rather than the proper substitution with Zr.

The effect of dopant size difference on Raman spectra of 2Y-TZP is shown in Figs. 7–9. 2Y-TZP doped with 0.5 mol% dopant shows six Raman modes in t-ZrO_2 (147, 260, 321, 465, 609, 640 cm^{-1}) as shown in Fig. 7. Fig. 8 shows that the stretching modes of Zr-O_{II} (260 cm^{-1}) and Zr-O_I (640 cm^{-1}) continuously shift to higher wavenumbers only when Sm_2O_3, Nd_2O_3, and La_2O_3 are added. A slight increase in the average bond length as a result of the increased substitution of dopant for Zr^{4+} should decrease the bond strength

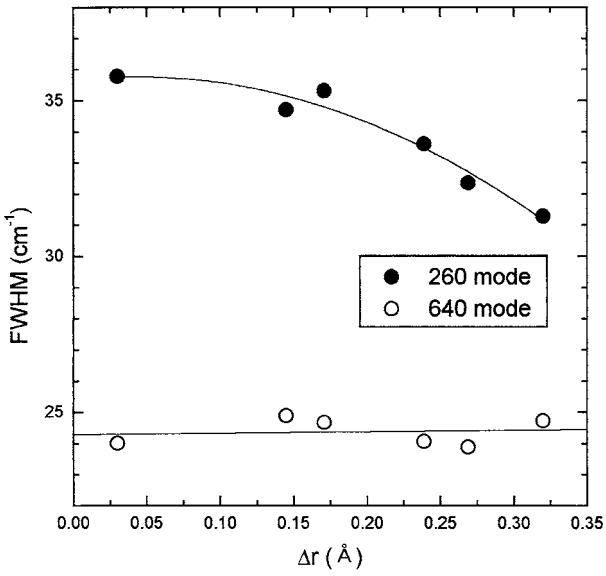

Figure 9 FWHM of 260 cm^{-1} mode and 640 cm^{-1} mode of 2Y-TZP doped with 0.5 mol% M_2O_3 (M = Sc, Yb, Y, Sm, Nd, La).

and consequently shift the Raman modes toward lower frequencies [10]. The irrelevancy is likely to arise because the influence of the decreased bond strength on the Raman modes may be annihilated by the formation of ordered structure. The variation of full width at half maximum (FWHM) of 260 cm^{-1} and 640 cm^{-1} modes of 2Y-TZP with 0.5 mol% dopant is shown in Fig. 9. FWHM of 640 cm^{-1} mode is almost constant, however, FWHM of 260 cm^{-1} mode decreases with increasing dopant ionic size, which indicates increased structural order with increasing dopant size. Therefore, as dopant ionic size is greater than Y^{3+}, the ordered structure such as pyrochlore phase ($A_2B_2O_7$) may be formed instead of c-ZrO_2, resulting in loss of phase stability.

4. Conclusions

As the trivalent cation was alloyed more than 0.5 mol%, the phase stability of t-ZrO_2 was maintained for Sc^{3+} doped 2Y-TZP, however, c-ZrO_2 was formed for those doped with Yb^{3+}, Y^{3+}, and Sm^{3+}, pyrochlore phase for those doped with Nd^{3+} and La^{3+}. Among trivalent cations, m-ZrO_2 concentration of the aged and the fractured 2Y-TZPs doped with Sc^{3+}, Yb^{3+}, and Y^{3+} firstly decreased and then increased due to loss of phase stability probably caused by the formation of pyrochlore phase when Sm^{3+}, Nd^{3+}, and La^{3+} were added. The decrease in FWHM of 260 cm^{-1} mode with increasing dopant ionic size indicated that structural ordered phase may be formed instead of c-ZrO_2 phase, representing that there may be a critical ionic size (0.239 Å) for phase stability in this system. For a given concentration of dopant, the dopant ionic size, therefore, is a function of phase stability.

Acknowledgement

This work was supported by Korea Research Foundation Grant (KRF-2000-041-F00275).

References

1. J. D. McCULLOUGH and K. N. TRUEBLOOD, *Acta. Crystallogr.* **12** (1955) 507.
2. D. Y. LEE, D.-J. KIM, D.-H. CHO and M.-H. LEE, *Ceram. Intl.* **24** (1998) 461.
3. P. LI, I.-W. CHEN and J. E. PENNER-HAHN, *J. Amer. Ceram. Soc.* **77** (1994) 118.
4. *Idem., ibid.* **77** (1994) 1281.
5. *Idem., ibid.* **77** (1994) 1289.
6. M. YOHIMURA and M. YASHIMA, *J. Mater. Sci.* **25** (1990) 2011.
7. R. C. GARVIE and P. S. NICHOLSON, *J. Amer. Ceram. Soc.* **55** (1972) 303.
8. M. J. MENDELSON, *ibid.* **52** (1969) 443.
9. D.-J. KIM, S.-H. HYUN, S.-G. KIM and M. YASHIMA, *ibid.* **77** (1994) 597.
10. D.-J. KIM, H.-J. JUNG and I.-S. YANG, *ibid.* **76** (1993) 2106.
11. R. D. SHANNON, *Acta Crystallogr.* **A32** (1976) 751.
12. A. V. SCHEVCHENKO, I. M. MALSTER and L. M. LOPATO, *Inorg. Mater.* **23** (1963) 1169.
13. A. ROUANET, *C. R. Acad. Sci.* **C267** (1968) 1583.
14. C. PASCUAL and P. DURAN, *J. Amer. Ceram. Soc.* **66** (1983) 23.
15. A. ROUANET and M. FORX, *C. R. Acad. Sci.* **C267** (1968) 874.
16. A. ROUANET, *Rev. Intl. Hautes Temp. Refract.* **8** (1971) 161.
17. J. LEFEVRE, *Ann. Chim. (Paris)* **8** (1963) 117.

Received 16 October 2000
and accepted 13 August 2001